THE ASTROPHYSICAL JOURNAL, 427:400–405, 1994 May 20

EVIDENCE OF CIRCUMSTELLAR MATTER SURROUNDING THE HERCULES X-1 SYSTEM

C. S. CHOI,[1] T. DOTANI,[2] F. NAGASE,[2] F. MAKINO,[2] J. E. DEETER,[3] AND K. W. MIN[4]
Received 1993 September 14; accepted 1993 November 23

ABSTRACT

We analyze data from two eclipse ingresses of Her X-1 observed with *Ginga* on 1989 April 30 and May 19. These observations occur, respectively, during the MAIN HIGH and SHORT HIGH states in the 35 day modulation of Her X-1 intensity. We find significant residual X-ray flux during eclipse, with a gradual decrease in flux following the occultation of the neutron star by the atmosphere of HZ Her. During the central part of the eclipse the count rate becomes nearly constant, at 0.5 mCrab in the energy range 1.7–36.8 keV. From a spectral analysis of the residual emission during the total eclipse of the central source in the MAIN HIGH state, we determine the energy spectral index, $\alpha = 0.8$, similar to that before eclipse. A remarkable feature of the eclipse spectrum is that it does not show a significant iron line feature in contrast to massive wind-fed pulsars, such as Vela X-1 and Cen X-3. From a timing analysis of the same eclipse data, we show that there are no pulses. These results imply that the emission comes from the scattering of continuum X-rays by material in a region considerably larger than the companion star. An extended accretion disk corona may be responsible for this scattering. However, partial eclipse of an extended accretion disk corona is insufficient to account for the count rates in mid-eclipse, when known parameters of the binary system are used. Based on the present results, we suggest that scattering occurs not only in the accretion disk corona but also in the circumstellar matter surrounding the system of Her X-1/HZ Her.

Subject headings: binaries: eclipsing — circumstellar matter — stars: individual (Hercules X-1) — stars: neutron — X-rays: stars

1. INTRODUCTION

Her X-1 is an eclipsing binary pulsar with a pulse period of 1.24 s and an orbital period of 1.7 days. It shows a 35 day quasi-periodic variation in X-ray intensity (Tananbaum et al. 1972) and pre-eclipse and anomalous absorption dips in certain orbital phases of the MAIN HIGH state (Crosa & Boynton 1980). The X-ray binary system Her X-1/HZ Her has the following stellar parameters: the companion star has mass $M_{opt} = 2.0\ M_\odot$ and radius $R_{opt} = 3.9\ R_\odot$, and the stellar separation is $a = 8.6\ R_\odot$ (Middleditch & Nelson 1976; Deeter, Boynton, & Pravdo 1981; Nagase 1989).

Most features of the 35 day cycle in Her X-1 are explained reasonably well by a tilted accretion disk counterprecessing with a 35 day period (Katz 1973; Petterson 1975, 1977; Gerend & Boynton 1976; Ögelman et al. 1985; Petterson, Rothschild, & Gruber 1991). In addition, an accretion disk corona (ADC) was proposed by Jones & Forman (1976) to explain the persistent low-state X-ray emission. Several low-mass X-ray binaries exhibit phenomena such as gradual and partial eclipses that might be explained by an ADC (Mason 1986, and references therein). A model of a partial eclipse of an ADC was first made for the X-ray light curve of 4U 1822−37 (White et al. 1981) and subsequently for 4U 2129+47 (White & Holt 1982).

An ADC around the central X-ray source is believed to be generated by the intense X-ray irradiation of matter that is flowing onto the accretion disk from the inner Lagrangian point or that is accreting onto the neutron star surface from the inner part of the accretion disk. Bai (1980) and Bochkarev (1989) suggested that the ADC above and below the accretion disk of Her X-1 is optically thin and hot and is in a highly ionized state (e.g., iron consists of He or H-like ions) due to the photoionization by the continuum X-rays from the neutron star. These models imply that the flux of scattered X-rays is very small compared with the direct component from the neutron star in a given high-intensity state of the 35 day cycle. Indeed, it is hard to decompose an observed spectrum into a scattered component and a direct one in a high-intensity state of Her X-1, except during the eclipse and the two dip phases (the pre-eclipse and anomalous dips).

Several results of spectral and timing analyses have previously indicated scattering by coronal gas in the Her X-1 system: (1) a soft component during the low-states of the 35 day cycle (Parmar et al. 1985; Mihara et al. 1991), (2) small residual flux during eclipses (Giacconi et al. 1973; Parmar, Sanford, & Fabian 1980; Parmar et al. 1985; Day, Tennant, & Fabian 1988; Mavromatakis 1993), and (3) an unpulsed residual component below 4 keV during the pre-eclipse dip of the MAIN HIGH state (Choi et al. 1994).

In addition to the ADC, Parmar et al. (1985) suggested that an additional scattering site, larger than the companion star, is needed to explain the emission observed at mid-eclipse during the MAIN HIGH state. According to their observation with the *EXOSAT* ME, the count rate at mid-eclipse is about 1 count s^{-1} in the energy range 2–10 keV. Most recently, Mavromatakis (1993) has observed mid-eclipse emission during the SHORT HIGH state of Her X-1 with *ROSAT*. Deeter et al. (1991) have reported an orbital period decrease at a rate of $\dot{P}_{orb}/P_{orb} = -1.32 \times 10^{-8}\ yr^{-1}$, which they conclude cannot be due to mass transfer through L_1 alone in a system that

[1] Korea Astronomy Observatory, 36-1 Whaam-dong Taejeon 305-348, Korea. E-mail: cschoi@apissa.issa.re.kr.
[2] The Institute of Space and Astronautical Science, 1-1 Yoshinodai 3-chome, Sagamihara, Kanagawa 229, Japan.
[3] Department of Astronomy FM-20, University of Washington, Seattle, WA 98195.
[4] Department of Physics, Korea Advanced Institute of Science and Technology, 373-1 Gusong-dong, Taejeon 305-701, Korea.

conserves mass and angular momentum. A highly ionized wind from the system may provide an extended scattering region and explain the observed orbital decay.

It was difficult to determine the X-ray spectrum of the scattered component by the corona in early X-ray observations, because of poor statistics at low X-ray intensity. In this paper we examine this spectrum with the relatively better *Ginga* statistics, using the data set taken at the phase of eclipse ingress of Her X-1, and deduce the presence of an extended scattering region. We present, in § 2, the X-ray light curve for the eclipse ingress phases observed at two different intensity levels (i.e., MAIN HIGH and SHORT HIGH) of the 35 day cycle. Two sample spectra, before and during the eclipse of MAIN HIGH are compared with each other in § 3. A test for pulsations during eclipse is also examined in § 3. In § 4 we summarize and discuss the results of our study.

2. OBSERVATIONS

Ginga observations covered most portions of the MAIN HIGH and SHORT HIGH states in the 35 day cycle of the binary X-ray pulsar Her X-1 (Deeter et al. 1994) with the large area counters (LAC) of total effective area of 4000 cm^2 (details are in Makino et al. 1987 and Turner et al. 1989) from 1989 April 26 to June 9. From those observations, we mainly analyzed two data sets that covered the orbital phase of eclipse ingress. A journal of these observations is given in Table 1.

For the MAIN HIGH state data observed on 1989 April 30, blank sky data in the vicinity of Her X-1, obtained 41–42 days before the observation, are used for background subtraction, with a periodicity of the non–X-ray background variation being taken into account. The dates of this background observation deviated 4–5 days from the 37 day periodicity in the variation reported by Hayashida et al. (1989). We checked the systematic error in background estimation introduced by this deviation and confirmed that the systematic error is much smaller than the statistical uncertainty of the eclipse data. In the case of the SHORT HIGH state data, however, we could not find an appropriate background observation, so we used the model background (see Hayashida et al. 1989).

The MAIN HIGH and SHORT HIGH states in a 35 day cycle last about 11 and 5 days, respectively (Tananbaum et al. 1972; Jones & Forman 1976). Data set I listed in Table 1 is obtained at the peak of the MAIN HIGH state. The total flux of this observation is about 16% larger than that of the high-intensity level obtained on 1988 August 28, in the range of 1.7–36.8 keV (Choi et al. 1994). A typical level of the SHORT HIGH state is about 30% of the flux of the MAIN HIGH state (Jones & Forman 1976; Deeter et al. 1994). The flux level of data set II corresponds approximately to a low-state level outside of eclipse. However, the observations one day earlier and one day later than the present observation of data set II recorded the typical flux level of the SHORT HIGH state. Therefore we conclude that data set II corresponds to a SHORT HIGH state. It appears that the pre-eclipse dip and the eclipse are smoothly connected in data set II (see Deeter et al. 1994).

Figure 1 shows that the detected count rates in both the MAIN HIGH and SHORT HIGH states tend to decrease gradually, after the neutron star enters into eclipse by being occulted by the atmosphere of the companion star HZ Her. From the light curve of MAIN HIGH state data, we roughly measure the transition time during which the neutron star passes through the companion star atmosphere to be about 100 s. The gradual and smooth decrease of X-ray intensity, even after the ingress transition, is apparent in the SHORT HIGH data. The timescale of the intensity decrease is about 37 minutes. Although the two states usually have a large difference in intensity level at the pre-eclipse phase ($\Phi_{orb} \approx 0.91$), they show similar count rates during the eclipses, as seen in Figure 1. The count rates near mid-eclipse are almost constant at a flux level of 0.5 mCrab in the energy range 1.7–36.8 keV. It is about a factor of 3 larger than the confusion limit of LAC (0.2 mCrab in the energy range 2–10 keV; Turner et al. 1989), and hence the flux is not due to a fluctuation of the X-ray background.

3. ANALYSIS AND RESULTS

We report here the analysis of data set I in which the spectral and pulse shape of the residual flux during the eclipse are examined in detail. We prefer to use data set I, since the background subtraction is more reliable than for data set II and the resulting spectrum can be interpreted with greater significance. Figure 2 shows two spectra from data set I obtained at the pre-eclipse (Fig. 2*a*) and eclipse (Fig. 2*b*) phases, respectively. The eclipse spectrum is acquired by summing data during the orbital phase $\Phi_{orb} = 0.932$–1.02.

To compare the two spectra in Figure 2, we calculate the count-rate ratios between observed spectra for individual pulse-height channels. Figure 3 shows such ratios for the two spectra in Figure 2, and for the spectrum of pre-eclipse dip

TABLE 1

OBSERVATIONS ON THE HER X-1 SYSTEM WITH THE *GINGA* SATELLITE

Data	Date (UT)	Φ_{orb}[a]	Ψ_{35}[b]	Flux Ratio[c]	Status
I	1989 Apr 30	0.90–1.02	0.120	1.156	MAIN HIGH
II	1989 May 19	0.90–0.97	0.656	0.025	SHORT HIGH

[a] The orbital phases are from the epoch reported by Deeter et al. 1991.

[b] The turn-on time is MJD 47,642.6 from the *Ginga* LAC observation.

[c] The total count-rate ratio (at $\Phi_{orb} \approx 0.91$) to that of the normal high-intensity level observed on 1988 August 28 in the energy range 1.7–36.8 keV.

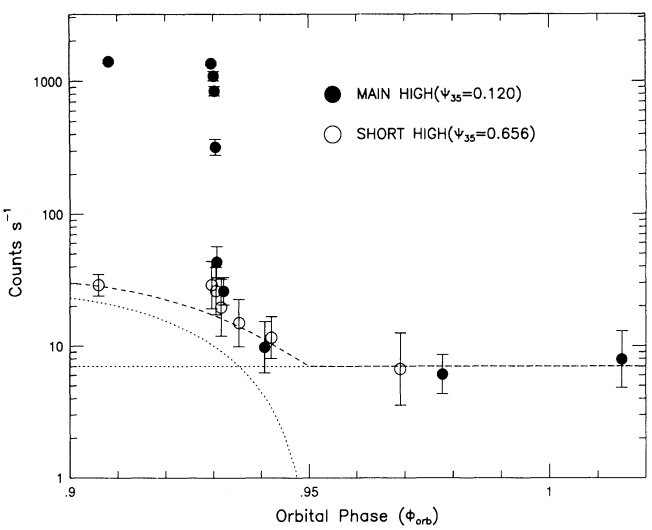

FIG. 1.—Light curve of Her X-1 in 1.7–36.8 keV, including eclipse ingress data observed on 1989 April 30 (*filled circles*) and May 19 (*open circles*), respectively. Dotted lines are two scattering components considered in the present study, and dashed line represents the sum.

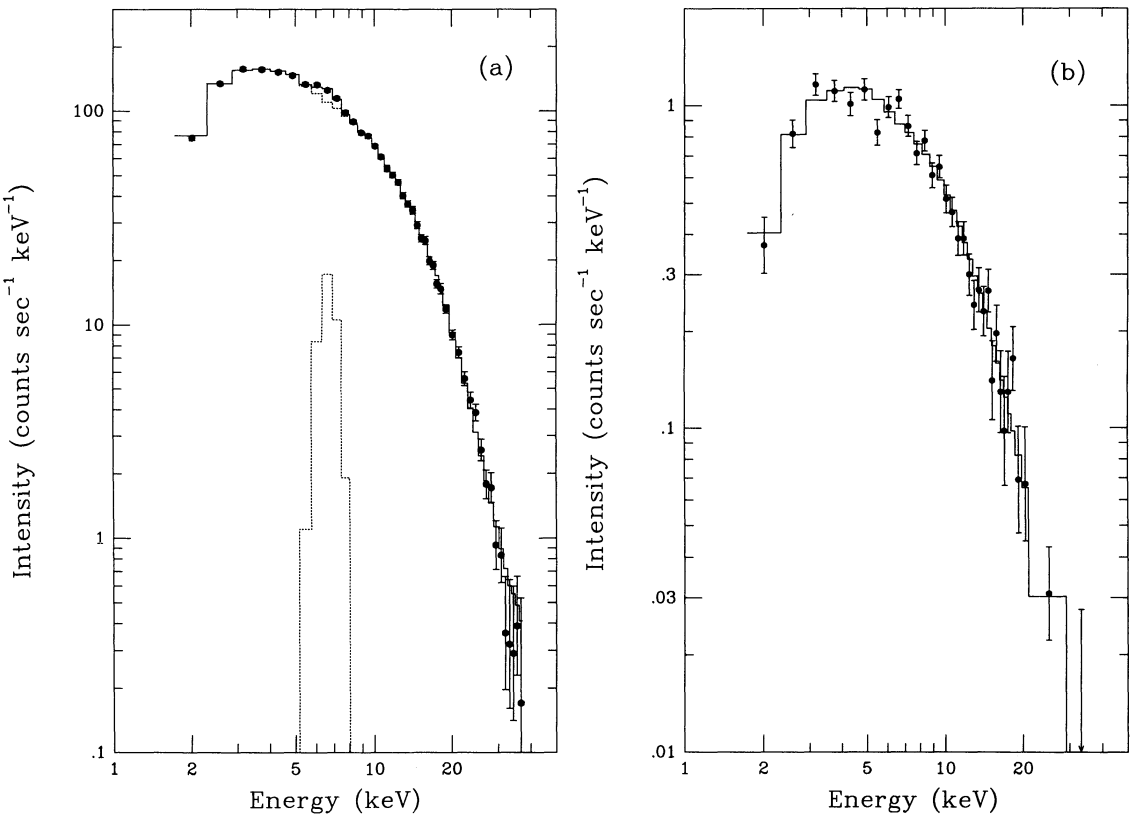

FIG. 2.—Energy spectra of Her X-1 calculated with data set I (*a*) at $\Phi_{orb} \approx 0.91$ and (*b*) during the eclipse. Best-fit model functions are plotted as a histogram. Energy spectra of (*a*) and (*b*) have almost the same shape.

state observed on 1988 August 28 (adopted from Choi et al. 1994). All three spectra have been normalized by a high-state spectrum also observed on 1988 August 28. According to Choi et al., the spectrum of the pre-eclipse dip contains a scattered component as well as a highly absorbed one. The scattered component is dominant at low energies (less than or equal to 4 keV) and is presumed to have the same spectral shape as that in the MAIN HIGH state. The flux observed during the eclipse is about 4 times lower than the scattered component in the pre-eclipse dip as seen in Figure 3.

3.1. *Features of the Eclipse Spectrum*

The high-level intensity spectrum of Her X-1 (Fig. 2*a*) is well reproduced with a typical model spectrum consisting of a power-law with an exponential high-energy cutoff (the form $H(E) = \exp\,[-(E - E_c)/E_f]$, for $E > E_c$, and $H(E) = 1$, for $E \leq E_c$, where E_c and E_f are the cutoff and the folding energies, respectively; see White, Swank, & Holt 1983) plus an iron emission line. As shown above, the eclipse and pre-eclipse spectra have almost the same spectral shape. So, we try to fit the two spectra with a conventional power-law model. The model spectrum adopted here is:

$$I(E) = A_1 E^{-\alpha} \exp\,(-\sigma N_H) H(E) + \frac{A_2}{\sqrt{2\pi}\Gamma} \exp\left(\frac{-(E - E_K)^2}{2\Gamma^2}\right), \quad (1)$$

where A_1, α, and N_H are the normalization coefficient of the continuum spectrum at 1 keV (in units of photons s^{-1} keV^{-1}), the power-law photon index, and the equivalent hydrogen column density (H-atoms cm^{-2}), respectively. For the interstellar/circumstellar absorption, we adopt the cross sections $\sigma(E)$ compiled by Morrison & McCammon (1983). The second term of equation (1) represents an iron line of Gaussian form, where A_2 is the iron line intensity in units of photons s^{-1}, E_K the line center energy, and Γ the intrinsic line width. In the present fitting we assumed a narrow line and fixed $\Gamma = 0.1$ keV. We did not apply absorption to the second term, because it is clear from Figure 2 that cold matter absorption has a negligible effect on the iron line intensity (see Mavromatakis 1993).

Using the above model, we have obtained acceptable fits for the spectra obtained before and during the eclipse of the MAIN HIGH state. The fitting results are summarized in Table 2, where the error and upper limit for each parameter is calculated for the 90% confidence level. Solid lines in Figures 2*a* and 2*b* represent the best-fit model spectra. We see that a simple power-law model can reproduce consistently the two spectra. In addition, the spectral indices shown in Table 2 indicate that the spectra are approximately the same, within statistical errors as expected from the pulse-height analyzer ratio analysis. In order to investigate other possibilities, we also tried to fit the eclipse spectrum with other emission models, for instance, a blackbody and a free-free emission. However, we could not obtain an acceptable fit with these models, in spite of the relatively poor statistics of the data.

There are no prominent spectral features associated with iron in the eclipse spectrum (i.e., absorption or fluorescent emission profiles of iron), and only an upper limit of iron line intensity of 0.43 photons s^{-1} and the equivalent width of

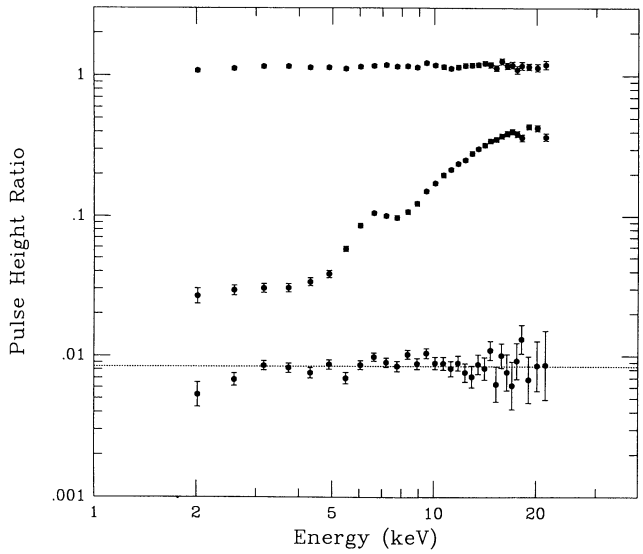

FIG. 3.—Pulse-height ratio spectra; from the top, the high-intensity level of data set I, the pre-eclipse dip state of 1988 August 28, and the eclipse state, respectively. The high-intensity level spectrum observed on 1988 August 28 is adopted from Choi et al. (1994) for the normalization.

EW $\leq$ 440 eV (listed in Table 2) can be determined at the 90% confidence level, where we fixed $E_K = 6.4$ keV for the eclipse spectrum. This upper limit means that the iron line emission at eclipse of Her X-1 is less than 2% of that of pre-eclipse. The equivalent hydrogen column density may indicate that a small amount of absorption is necessary for the eclipse spectrum. At present, it is not possible to provide a clear answer for the origin of the absorption. However, it seems that the two data points in the lowest energy of the spectrum affect the fitting (see Fig. 3). This will be discussed in § 4.

3.2. *No Pulsation from Residual Fluxes during Eclipse*

The eclipse spectrum for Her X-1 is very similar to the high-state spectrum, so it is possible that pulsations might also be present in the light curve during eclipse. To test for this possibility, we extract a pulse amplitude for the residual counts during the eclipse state in data set I using a pulse-folding technique. We fixed the pulse period to $P = 1.237757$ s, which is adopted from Deeter et al. (1991), after correction of the binary motion of Her X-1.

The pulse amplitude A_{mp} is estimated using the following equation,

$$A_{mp} = \frac{1}{\bar{x}} \left\{ \frac{\sum_i [(x_i - \bar{x})^2 - \sigma_i^2]}{N} \right\}^{1/2}, \quad (2)$$

where x_i, $\bar{x}$, σ_i, and N are the count rate of the ith bin, the phase-averaged count rate, the statistical fluctuation of count rate, and the number of bins ($N = 20$), respectively. From this analysis, we can place a 90% upper limit to the pulse amplitude at 20% of the residual flux in the energy range of 1.6–36.8 keV. Note that this upper limit is much smaller than the pulse amplitude at pre-eclipse which is 65% (see Choi et al. 1994).

4. DISCUSSION

4.1. *Eclipsing Behavior*

We have analyzed data for two eclipse ingresses of Her X-1 obtained from the *Ginga* observations made on 1989 April 30 and May 19. From the light curve of MAIN HIGH state data, we measure the transition time during which the neutron star passes through the companion star atmosphere to be about 100 s. This duration agrees with that of egress reported by Day et al. (1988), except for one unusual long egress in their data. Unfortunately, it is not possible to compare the duration between eclipse ingress and egress, since *Ginga* did not cover egresses in the observations. Thus we shall confine our discussion here to the ingresses. If we adopt a combined orbital velocity for the neutron star and the companion star of $V_{orb} \approx 285$ km s^{-1} (see, e.g., Deeter et al. 1981), the extent of the atmosphere of HZ Her is $\sim 3 \times 10^9$ cm, assuming an inclination angle close to $i = 90°$. The steep intensity drop for the MAIN HIGH data (Fig. 1) is evidently due to photoelectric absorption by the atmosphere. The direct beam should not be seen after the neutron star has been eclipsed following ingress.

In addition to the sharp decrease associated with the ingress of the neutron star, the intensity behavior of the source (see Fig. 1) shows the following notable features described in § 2: (1) light curves of both the MAIN HIGH and SHORT HIGH states show a very similar pattern of a smooth and gradual decline, (2) the count rates near mid-eclipse level off at a nonzero, definite value, confirming the residual mid-eclipse emission observed with *EXOSAT* by Parmar et al. (1985) and with *ROSAT* by Mavromatakis (1993). The calculated mid-eclipse flux is $(2.0 \pm 0.2) \times 10^{-11}$ ergs cm^{-2} s^{-1} in the energy range 2–10 keV. The gradual decrease supports the presence of an extended emission region, which has been proposed to explain the low-state X-ray emission (Jones & Forman 1976; Parmar et al. 1985; Mihara et al. 1991). From the time interval of this gradual eclipse ($\approx$37 minutes), we infer that the emission region extends at least over a radius $r \sim 6 \times 10^{10}$ cm from the neutron star, where we assume the emission region is symmetric. This is comparable to the extent of the disk ($\sim 10^{11}$ cm; Howarth & Wilson 1983).

According to the disk precession model of Her X-1, the 35 day intensity modulation is caused by the relative orientation of the accretion disk to the observer. In spite of the large modulation in intensity outside of eclipse, the detected X-rays during eclipse of the central source are independent of the 35 day intensity modulation. It seems that the extended X-ray

TABLE 2

BEST-FIT PARAMETERS FOR THE TWO SPECTRA OF MAIN HIGH[a]

Number[b]	A_1[c]	α	log N_H	A_2[d]	E_K[e]	EW[f]	χ^2_ν (d.o.f.)
1	621.6 ± 34.8	0.87 ± 0.03	≤21.5	24.5 ± 5.5	6.62 ± 0.15	200 ± 50	0.89 (38)
2	4.41 ± 0.30	0.80 ± 0.04	22.03 ± 0.20	≤0.43	...	≤440	1.17 (28)

[a] Quoted errors and upper limits are 90% confidence level for each parameter.
[b] Items correspond to the spectra of Figs. 2*a* and 2*b*, respectively.
[c] Normalization A_1 of continuum in units of photons s^{-1} keV^{-1}.
[d] Line intensity A_2 in units of photons s^{-1}.
[e] Iron line energy E_K is in units of keV.
[f] Equivalent width EW is in units of eV.

emission region always exists in the Her X-1 system with more or less stable conditions.

4.2. *Two Scattering Components*

In the previous section, we found no pulsation for the eclipse data. This absence of pulsation, together with the presence of residual flux during the mid-eclipse and the spectral similarity shown in Table 2, strongly suggests the emission during eclipse is due to scattering by an extended region. The possible contribution from the scattering by interstellar dust is negligible, since Her X-1 is located at a relatively high galactic latitude ($l = 58.^{\circ}23$, $b = 37.^{\circ}42$). Hence we consider hereafter the scattering by circumstellar matter in the binary system.

It was noted in § 3.1 that the flux level during eclipse is about one-fourth of that of the unpulsed residual count (in the low energy) detected during the pre-eclipse dip. This means that 75% of the scattering region is obscured by the companion star, if we apply a partial eclipse model in which the scattered flux from the ADC (assumed homogeneously distributed) is intercepted partly by the companion star.

However, this model is insufficient to explain the residuals represented by the three data points near mid-eclipse in Figure 1, even with the ADC extending to the Roche lobe radius $r \approx 2 \times 10^{11}$ cm, since it would be expected that the companion star ($r_c \approx 3 \times 10^{11}$ cm) blocks out almost all of the extended corona at around the midpoint of eclipse. It should be noted that the Her X-1 system has a high inclination angle $i \geq 85^{\circ}$ (Deeter et al. 1981; Nagase 1989). The three data near mid-eclipse (Fig. 1) indicate that there is an almost constant flux persisting during the central part of the eclipse. We take this as evidence for another scattering component. The dotted lines shown in Figure 1 represent the two scattering components considered in the present study. The gradual decrease of observed flux can be understood as being caused by the shielding of the ADC (Fig. 1, *dotted curve*), as the neutron star ingresses into eclipse. Such a component becomes negligible as the eclipse progresses, so that the contribution from the persistent scattering component (*dotted flat curve*) appears.

We consider two possible sites for producing the persistent emission. The first one is the atmosphere of HZ Her. Using our determination of 3×10^9 cm for the size of the atmosphere, we estimate the solid angle subtended by the cross-sectional area of the envelope is $\Omega \sim 10^{-3}$ sr as seen from the neutron star. However, this value is too small to give the observed count rates, because it needs a large amount of column density $N_{\rm H} \approx 8 \times 10^{-3}(4\pi/\Omega)/\sigma_{\rm T} \sim 10^{26}$ cm^{-2}—where $\sigma_{\rm T}$ is the Thomson scattering cross section—which is inconsistent with the small amount of absorption obtained by the model fitting to the spectrum. The other possible site is circumstellar matter encompassing the binary system, possibly being lost from the system by mass flow from the accretion disk or the companion star.

4.3. *Mass Loss from the System*

We consider here the possibility that scattering by a continuous mass outflow from the Her X-1 system is responsible for the eclipse emission at about 0.8% of the direct X-ray emission outside eclipse. This amount of circumstellar scattering to an observer requires a column density of $N_{\rm H} \approx 1 \times 10^{22}$ cm^{-2} assuming an isotropic wind emanating from the system and isotropic X-ray emission from Her X-1. Incidently, the absorption column of the eclipse spectrum listed in Table 2 is consistent with this value. The finite value of $N_{\rm H}$ in the eclipse spectrum may be due to self-absorption in the scattering gases. However, the small level of absorption in the high-state spectrum contradicts this possibility. According to the *ROSAT* observation by Mavromatakis (1993), the interstellar/circumstellar column density toward Her X-1 is on the order of 10^{20} cm^{-2}. This fact implies that the scatterer is highly ionized. Therefore the finite amount of absorption obtained from the model fitting to the mid-eclipse spectrum may be due to the systematic error introduced by the background subtraction.

Several theoretical mechanisms have been investigated for mass ejection from X-ray binary systems: e.g., X-ray induced stellar winds (Davidson & Ostriker 1973; Arons 1973; London & Flannery 1982; London, Flannery, & Auer 1981) and winds driven from an accretion disk irradiated by X-rays (Begelman et al. 1983a, b, and references therein). The expected mass-loss rate is $\dot{M} \approx 10^{-8}\ M_{\odot}$ yr^{-1} for the stellar wind model and $\dot{M} \approx 10^{-8}$–$10^{-7}\ M_{\odot}$ yr^{-1} for the disk wind model.

If we assume that distribution of the winds emanating from the Her X-1 system is spherically symmetric with respect to the neutron star, we could express the mass-loss rate as

$$\frac{dM}{dt} = \int n_w v_w \, dA = \frac{4\pi R^2 N_{\rm H} \mu m_{\rm H} v_w}{\int_R^{\infty} f(r) dr}, \qquad (3)$$

where n_w, $N_{\rm H}$, μ, $m_{\rm H}$, and v_w are the density of the wind at distance r from the neutron star (we assume the radial density profile $n_w(r) = n_w(R) f(r)$ for $r > R$; R is the Roche lobe radius of the neutron star), the radial hydrogen column density, the mean molecular weight of the gas, the hydrogen mass, and the wind velocity at R, respectively. With the column density calculated previously, we estimate the mass-loss rate as roughly $\dot{M} \sim 3 \times 10^{-8}\ M_{\odot}$ yr^{-1}, when we assume that the density profile and the wind velocity are $f(r) = (R/r)^2$ and $v_w = 1000$ km s^{-1} (about twice the escape velocity), respectively. The necessary density profile $f(r)$ and magnitude of the wind velocity v_w are not unreasonable. The mass-loss rate could be explained either by X-ray–induced stellar winds from the companion atmosphere or by a Compton-heated wind from the accretion disk. As the density of such wind at R is estimated to be $n_w(R) \sim 9 \times 10^{10}$ cm^{-3}, the ionization parameter $\xi = L_x/[n_w(R)R^2] \sim 10^4$. This means that most of the wind that causes the scattering is highly ionized and therefore that the matter does not absorb soft X-rays. However, the wind that is close to the X-ray shadow of HZ Her may have a lower ionization parameter (see discussion on the X-ray ionized winds of massive X-ray binaries by Hatchett & McCray 1977) and could cause absorption similar to that reported here.

From the present analysis of the two eclipse transitions, we summarize the findings as follows: (1) The light curve shows that the X-ray intensity, after passing across the atmospheric occultation by the companion star, decreases gradually. This indicates that an extended emission region, probably an ADC, exists in the Her X-1 system, as has been suggested by several authors. The light curves are almost the same at two different intensity levels of the SHORT HIGH and the MAIN HIGH state. (2) There exists a small amount of residual flux ($\sim$0.5 mCrab) at mid-eclipse, confirming the previous *EXOSAT* and *ROSAT* observations. It is hard to explain such persistent emission by the partial eclipse model of ADC, which is highly ionized and can be extended only up to $r \sim 10^{11}$ cm, with known orbital parameters. (3) The shape of the eclipse spectrum (power index $\alpha = 0.8$) is found to be very similar to that of the continuum

X-rays at the high-intensity state, within statistical errors. This implies that the X-ray emission during the eclipse is scattered flux of the direct beam by an extended source. There is no significant iron line feature. (4) No evidence of pulsation is found for the emission remaining during total eclipse of the neutron star. (5) It is suggested that a second extended source surrounds the Her X-1/HZ Her system, which accounts for the scattered flux observed during the total eclipse. This source could be either X-ray–induced stellar winds from the companion atmosphere or a wind driven from the accretion disk irradiated by X-rays.

The authors wish to express their gratitude to Prof. A. C. Fabian for his helpful comments on the manuscript. C. S. C. is grateful to the Korea Astronomy Observatory for supporting his visit to Japan, and also to the Japan Society for Promotion of Science for a research fellowship. The contribution by J. E. D. was supported by NASA grant NAG 8-207.

REFERENCES

Arons, J. 1973, ApJ, 184, 539
Bai, T. 1980, ApJ, 239, 328
Begelman, M. C., & McKee, C. F. 1983a, ApJ, 271, 89
Begelman, M. C., McKee, C. F., & Shields, G. A. 1983b, ApJ, 271, 70
Bochkarev, N. G. 1989, Soviet Astron., 33, 638
Choi, C. S., Nagase, F., Makino, F., Dotani, T., & Min, K. W. 1994, ApJ, 422, 799
Crosa, L. M., & Boynton, P. E. 1980, ApJ, 235, 999
Davidson, K., & Ostriker, J. P. 1973, ApJ, 179, 585
Day, C. S. R., Tennant, A. F., & Fabian, A. C. 1988, MNRAS, 231, 69
Deeter, J. E., Boynton, P. E., Miyamoto, S., Kitamoto, S., Nagase, F., & Kawai, N. 1991, ApJ, 383, 324
Deeter, J. E., Boynton, P. E., & Pravdo, S. H. 1981, ApJ, 247, 1003
Deeter, J. E., Scott, D. M., Boynton, P. E., Miyamoto, S., Kitamoto, S., Takahama, S., & Nagase, F. 1994, ApJ, in press
Gerend, D., & Boynton, P. E. 1976, ApJ, 209, 562
Giacconi, R., Gursky, H., Kellogg, E., Levinson, R., Schreier, E., & Tananbaum, H. 1973, ApJ, 184, 227
Hatchett, S., & McCray, R. 1977, ApJ, 211, 552
Hayashida, K., et al. 1989, PASJ, 41, 373
Howarth, I. D., & Wilson, B. 1983, MNRAS, 202, 347
Jones, C., & Forman, W. 1976, ApJ, 209, L131
Katz, J. I. 1973, Nature Phys. Sci., 246, 87
London, R. A., & Flannery, B. P. 1982, ApJ, 258, 260
London, R. A., Flannery, B. P., & Auer, L. H. 1981, ApJ, 243, 970
Makino, F., & Astro-C Team. 1987, Ap. Lett. Comm., 25, 223
Mason, K. O. 1986, in The Physics of Accretion onto Compact Object, ed. K. O. Mason, M. G. Watson, & N. E. White (New York: Springer), 29
Mavromatakis, F. 1993, A&A, 273, 147
Middleditch, J., & Nelson, J. 1976, ApJ, 208, 567
Mihara, T., Ohashi, T., Makishima, K., Nagase, F., Kitamoto, S., & Koyama, K. 1991, PASJ, 43, 501
Morrison, R., & McCammon, D. 1983, ApJ, 270, 119
Nagase, F. 1989, PASJ, 41, 1
Ögelman, H., Kahabka, P., Pietsch, W., Trümper, J., & Voges, W. 1985, Space Sci. Rev., 40, 347
Parmar, A. N., Pietsch, W., McKechnie, S., White, N. E., Trumper, J., Voges, W., & Barr, P. 1985, Nature, 313, 119
Parmar, A. N., Sanford, P. W., & Fabian, A. C. 1980, MNRAS, 192, 311
Petterson, J. A. 1975, ApJ, 201, L61
———. 1977, ApJ, 218, 783
Petterson, J. A., Rothschild, R. E., & Gruber, D. E. 1991, ApJ, 378, 696
Tananbaum, H., Gursky, H., Kellogg, E. M., Levinson, R., Schreier, E., & Giacconi, R. 1972, ApJ, 174, L143
Turner, M. J. L., et al. 1989, PASJ, 41, 345
White, N. E., Becker, R. H., Boldt, E. A., Holt, S. S., Serlemitsos, P. J., & Swank, J. H. 1981, ApJ, 247, 994
White, N. E., & Holt, S. S. 1982, ApJ, 257, 318
White, N. E., Swank, J. H., & Holt, S. S. 1983, ApJ, 270, 711